

Atomic oxygen chemisorption on the sidewall of zigzag single-walled carbon nanotubes

Vl. A. Margulis*

Department of Physics, N. P. Ogarev Mordovian State University, Saransk 430000, Russia

E. E. Muryumin

Department of Chemistry, N. P. Ogarev Mordovian State University, Saransk 430000, Russia

(Received 29 August 2006; revised manuscript received 2 December 2006; published 31 January 2007)

A theoretical approach is developed to study the chemisorption of a single oxygen atom on the outer surface of zigzag single-walled carbon nanotubes (ZSWCNTs). The adatom Green's function, the charge transfer between the nanotubes and the chemisorbed O atom, and the adsorption energy ΔE_{ads} are calculated within the Anderson-Newns model, which takes account of Coulomb interaction between adsorbate electrons. Two different adsorption positions are considered, in which an oxygen atom forms a bridge between two nearest-neighbor carbon atoms: one is on top of an axial C-C bond (position I), and the other—on top of a zigzag C-C one (position II). According to our calculations carried out for a series of the ZSWCNTs $(p,0)$ with p ranging from 9 to 18, the adsorption of a single O atom in both the above-mentioned positions is possible and equally probable from the energetic point of view as the corresponding adsorption energies, being negative, are almost identical. The absolute values of these energies generally fall into the range 1.1–2.7 eV, larger $|\Delta E_{\text{ads}}|$ values being associated with semiconducting tubes. For the latter ones, ΔE_{ads} is found to be practically independent of the nanotube radius R , whereas for metallic tubes ΔE_{ads} slightly decreases with increasing R , tending towards the “infinite” radius graphene case. The localized acceptor states created by the O adatom in the band gap of the semiconducting ZSWCNTs are found to be responsible for such a different behavior of ΔE_{ads} as a function of R for the two types of nanotubes (metallic and semiconducting), as well as for the lowering in ΔE_{ads} (by about 0.5 eV) for the semiconducting tubes as compared with the metallic ones. It is also shown that a fairly large charge transfer (of about 0.55 electron) to the O adatom occurs when it is chemisorbed on the outer surface of the ZSWCNTs, which suggests that their electronic transport properties can be significantly changed upon chemisorption of atomic oxygen.

DOI: [10.1103/PhysRevB.75.035429](https://doi.org/10.1103/PhysRevB.75.035429)

PACS number(s): 61.46.–w, 68.43.–h

I. INTRODUCTION

The use of foreign atoms and molecules for functionalization of carbon nanotubes (CNTs) is a subject of considerable current interest, since it is expected that a variety of novel nanodevices can be produced in such a way (for a recent review of the development of the subject, see Ref. 1). In this context, the adsorption of oxygen on CNTs is of particular interest. As it was shown in the pioneering works,^{2–4} exposure of single-walled carbon nanotubes (SWCNTs) to air or oxygen can have a dramatic effect on their electronic transport properties, although several subsequent works (see, e. g., Refs. 5–10) suggest that the observed behaviors are probably not due to the direct interaction of oxygen with the nanotubes. A number of theoretical studies have also been reported on the physisorption of oxygen molecules,^{11–26} as well as on the chemisorption of single oxygen atoms,^{24–29} on the surface of SWCNTs. Most of these studies have primarily employed first-principles calculations based on the density functional theory in the attempt to identify the preferable adsorption sites and to predict the adsorption energies. These calculations, however, are computationally very expensive and have, therefore, so far been limited to only a few selected prototype nanotubes of fairly small diameters, modeled by supercells of about one hundred carbon atoms at most. Furthermore, in spite of the qualitative resemblance of some of the conclusions made in Refs. 11–29, the results reported by different authors regarding the oxygen adsorption energies are markedly different and apparently depend

on the approximations used. This indicates that further theoretical developments are still necessary before obtaining a quantitative view on this problem.

The key issue one desires to elucidate is how the electronic structure of SWCNTs affects their adsorption properties in regard to molecular and atomic oxygen. Since a first-principles study of the problem is a formidable task, a more simple, easy-to-handle approach to the theory of oxygen adsorption on SWCNTs, amenable to analytical treatment, might be useful for practical purposes as well as for a clear understanding of the factors that determine the adsorption properties of the nanotubes.

Recently, we have proposed such an approach for studying the chemisorption of single atoms on the outer surface of SWCNTs.³⁰ The approach is similar to that originally developed by Newns³¹ to describe hydrogen chemisorption on transition metal surfaces and is based on the Anderson model for dilute magnetic impurities in metals.³² The advantage of this approach is that it captures some essential features of the physics of chemisorption, allowing the origins of systematic chemisorption-energy trends to be established. The disadvantage of the approach is that a number of phenomenological parameters are incorporated in the theory, which cannot be calculated within the context of the model and should be reasonably chosen in some or other way (for example, by adjusting to give the best fit to even one experimentally derived binding energy). If the problem of the parametrization of the model is resolved, then the approach is sufficiently flexible and effective from a computational point of view.

While for the reason indicated above the approach cannot be expected to yield accurate results for adsorption energies, it can be very useful for studying the effect of the various relevant parameters of the system under consideration on its adsorption properties. In Ref. 30, a model calculation within this approach has been implemented for an individual H atom adsorbed on the sidewall of different zigzag SWCNTs (ZSWCNTs) in the atop position, i.e., directly above a surface carbon atom. Despite the simplicity of the model used in that paper, it did provide a qualitative understanding of the main physical features of atomic hydrogen chemisorption on the ZSWCNTs.

It is our objective in the present paper to extend the approach based on the Anderson-Newns model to deal with oxygen adatoms, which, as well documented by the *ab initio* studies quoted above, prefer to be adsorbed on top of C-C bond in a bridge configuration. We illustrate this extension with a systematic study, the first to our knowledge, of the chemisorption of a single O atom on the sidewall of a number of ZSWCNTs with somewhat large diameters. The emphasis is put on revealing the interplay between the intrinsic electronic and adsorption properties of the nanotubes. For this purpose we also explore the charge transfer that accompanies the chemical bonding of an oxygen atom to a SWCNT.

The remainder of the paper is divided as follows. In the next section, we describe the model used and develop a formal approach to the problem, which is based on the Green's-function method. In Sec. III, we present numerical results obtained with parameters appropriate to atomic oxygen chemisorption on a series of ZSWCNTs $(p,0)$ with p ranging from 9 to 18. Finally, a brief summary of the findings is given in the last section.

II. MODEL AND FORMALISM

The system under consideration consists of a perfect ZSWCNT with an individual oxygen atom adsorbed on its sidewall. In the spirit of the approach proposed by Anderson³² and Newns,³¹ the adatom is modelled by a single relevant electronic level with energy ε_a (hereafter, all energies are measured from the Fermi level of the substrate nanotube), the corresponding eigenfunction $\Psi_{a\sigma}(\mathbf{r}) \equiv |a\sigma\rangle$ (σ denotes the electron spin) being not specified precisely. When the adatom interacts with the substrate, an electronic charge is generally transferred from the substrate to the adatom (or vice versa). Consequently, it is necessary to take account of the Coulomb repulsion U between the electrons on the adatom and to consider the occupancy $\langle n_{a\sigma} \rangle$ of the adatom level. It should be noted that the conventional Anderson-Newns model formally ignores Coulomb interactions between adatom electrons and substrate ones. However, according to Lyo and Gomer,^{33,34} the interaction between them can be roughly taken into account in terms of the effective image potential $V_{\text{im}}^{\text{eff}}$ (defined as a positive quantity), which renormalizes ε_a and U so that the effective adatom level of spin σ is shifted to

$$E_{a\sigma} = \varepsilon_a + V_{\text{im}}^{\text{eff}} + (U - 2V_{\text{im}}^{\text{eff}})\langle n_{a-\sigma} \rangle, \quad (1)$$

where $\langle n_{a-\sigma} \rangle = \langle c_{a-\sigma}^\dagger c_{a-\sigma} \rangle$ is the expected occupancy of the adatom by an electron of spin $-\sigma$ (c^\dagger and c are Fermi cre-

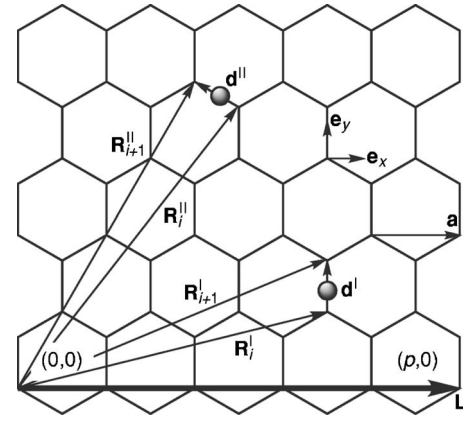


FIG. 1. Fragment of a two-dimensional graphite sheet which is rolled up in order to construct a ZSWCNT specified by an index $(p,0)$. The unit vectors denoted by \mathbf{e}_x and \mathbf{e}_y are directed along the circumference and the axis of the nanotube, respectively. Also shown a chiral vector \mathbf{L} corresponding to the circumference of the tube and one of the primitive translation vectors of the lattice structure of a graphene plane, denoted by \mathbf{a} . The grey balls schematically show two possible stable adsorption positions of an oxygen atom on the surface of a SWCNT (for details, see the text). The vectors labeled \mathbf{R}_i and \mathbf{R}_{i+1} are the position vectors of two surface nearest neighbors of the adatom, which are connected by vector \mathbf{d} . The superscripts I and II refer to the two abovementioned positions of the adatom.

ation and annihilation operators, respectively). It seems reasonable to treat $V_{\text{im}}^{\text{eff}}$, which plays a nontrivial role in determining the adsorption energy, as a phenomenological parameter, since the classical result for the image potential energy $V_{\text{im}} = q^2/4z$ of a point charge q at a distance z from the flat surface is not valid when the adatom is brought very close to the surface (see the discussion in Ref. 34). In any case the image potential for the cylindrical geometry of a SWCNT is significantly more complicated than that of the planar configuration.^{35,36}

We next turn to the consideration of a substrate ZSWCNT $(p,0)$ forming a cylinder of length A and perimeter L . According to Fig. 1, this geometry is constructed from a strip-shaped graphite layer by wrapping it in the lateral direction specified by a circumference vector $\mathbf{L} = p\mathbf{a}$, where $\mathbf{a} = a_0(1,0)$ in the Cartesian coordinates (x,y) with the x direction along the circumference and the y direction along the axis of the nanotube (a_0 is the lattice constant of the graphite).

The simplest possible framework to treat the electronic structure of SWCNTs is a $\mathbf{k} \cdot \mathbf{p}$ two-band model within an effective-mass approximation.³⁷ This model has the advantage that one can find simple analytical expressions for the energy bands and the corresponding eigenstates (see further below), which are valid in the vicinity of K and K' points at the corners of the hexagonal Brillouin zone of a graphene sheet rolled up into a SWCNT (for a detailed discussion of the nanotube band structure and unit cells, see Ref. 38). However, since the energy bands are, thereby, obtained from the zone-folded graphene π -orbital bands, the effects caused

by the finite tube curvature (such as σ - π hybridization and the misalignment of the π orbitals at nearest-neighbor carbon atoms) are left out of account in the model. These effects are negligibly small for SWCNTs of somewhat large diameters (more than, say, 1 nm), and it is, therefore, not surprising that the above-mentioned model has been used in many papers (for a review, see Ref. 39), successfully predicting a number of the key properties of such nanotubes. The model seems to be sufficient for studying the chemisorption problem as well, and it is this model that we are going to use further.

Within the band model of ZSWCNTs we have adopted, the energy bands, which are located near the K point, are given by^{37,39}

$$\varepsilon_{\nu\lambda}^{(K)} = s(\varepsilon_{\nu m}^2 + \gamma^2 k^2)^{1/2} \quad (2)$$

with the composite index $\lambda = (m, s, k)$ and

$$\varepsilon_{\nu m} = \gamma \kappa_{\nu m} = \eta(3m - \nu), \quad \eta = \gamma/3R, \quad (3)$$

where the index $\nu (=0, \pm 1)$ is specified via the relation $p = 3M + \nu$ with integer M ($\nu=0$ for metallic ZSWCNTs and $\nu=\pm 1$ for semiconducting ones), $m=0, \pm 1, \pm 2, \dots, \pm(p-1)$ is an index that labels size-quantized energy subbands arising due to the quantization of the transverse electron wave vector $\kappa_{\nu m}$ in the circumference direction, $s=\pm 1$ stands for the band index (the upper and lower signs refer to the conduction and valence bands, respectively), k is the one-dimensional wave vector along the tube axis, $\gamma = \sqrt{3}|V_{pp\pi}|a_0/2$ is the $\mathbf{k} \cdot \mathbf{p}$ interaction parameter ($V_{pp\pi}$ is the transfer integral between π orbitals of the nearest-neighbor carbon atoms), and R is the nanotube radius. The energy bands associated with the K' point are obtained by the replacement $\nu \rightarrow -\nu$ in Eq. (2).

With the systematics summarized above, we now proceed to the chemisorption problem. When the adatom is placed at a short distance from the substrate ZSWCNT, the overlap between the atomic $\Psi_{a\sigma}(\mathbf{r})$ and the substrate $\Psi_{\nu\lambda\sigma}(\mathbf{r})$ wave functions gives rise to the chemisorption bonding. A schematic representation of this situation is provided by an Anderson-Newns type of Hamiltonian

$$H^{(\nu)} = \sum_{\lambda\sigma} \varepsilon_{\lambda\sigma} c_{\lambda\sigma}^\dagger c_{\lambda\sigma} + \sum_{\sigma} E_{a\sigma} c_{a\sigma}^\dagger c_{a\sigma} + \sum_{\lambda\sigma} (V_{a\sigma, \nu\lambda\sigma} c_{a\sigma}^\dagger c_{\lambda\sigma} + \text{H.c.}), \quad (4)$$

where $c_{\lambda\sigma}^\dagger$ ($c_{\lambda\sigma}$) creates (destroys) an electron of spin σ in the state $|\nu\lambda\sigma\rangle \equiv \Psi_{\nu\lambda\sigma}(\mathbf{r})$ of the substrate ZSWCNT, and $V_{a\sigma, \nu\lambda\sigma}$ is the configuration interaction, as referred to by Fano.⁴⁰ This interaction is represented by a nondiagonal matrix element of the effective self-consistent Hartree-Fock potential $V(\mathbf{r} - \mathbf{R}_a)$ of the entire (substrate plus adatom) system as follows:

$$V_{a\sigma, \nu\lambda\sigma}(\mathbf{R}_a) = \int \Psi_{a\sigma}^*(\mathbf{r}) V(\mathbf{r} - \mathbf{R}_a) \Psi_{\nu\lambda\sigma}(\mathbf{r}) d^3r, \quad (5)$$

where $\mathbf{R}_a(0, 0, z_a)$ denotes the position of the adatom and the origin of the coordinate system is placed at a point on the surface of the ZSWCNT directly below the adatom. The presence of the potential $V(\mathbf{r} - \mathbf{R}_a)$ in Eq. (5) suggests that all the electrons of the system are, at least in principle, involved in the formation of one chemisorption bond between the adatom and the nanotube.

In our earlier paper,³⁰ the matrix element of this type has been evaluated in the case of a single adatom placed directly above a surface carbon atom, i.e., in the atop position. It is not expected to occur in the case of atomic oxygen chemisorption on SWCNTs. The results of *ab initio* and semi-empirical calculations²⁴⁻²⁹ show unambiguously that an oxygen atom is adsorbed on a SWCNT preferably on top of the C-C bond, forming a bridge configuration analogous to an organic epoxide. Two nonequivalent stable bridge positions, which we shall further refer to as positions I and II, have, thereby, to be clearly distinguished. In position I the vector \mathbf{d} connecting the two surface nearest neighbors of an adatom is parallel to the tube axis, while in position II the angle between them is 60° . Figure 1 illustrates our labeling convention for adsorption sites marked with grey balls sitting symmetrically between two substrate carbon atoms. An adatom electron can hop to any of them, resulting in the bridge binding we focus our attention on here.

To proceed further, it is convenient to express the electron wave function $\Psi_{\nu\lambda\sigma}(\mathbf{r})$ for the energy bands associated with the K point in terms of the Wannier functions $\Phi(\mathbf{r} - \mathbf{R}_i)$, which realize the site representation of electronic states. With the Bloch function at the K point expressed in the form of a linear combination of the Wannier functions, we have

$$\Psi_{\nu\lambda\sigma}(\mathbf{r}) = F_{\nu\lambda}(\mathbf{r}) \chi_\sigma \frac{1}{\sqrt{N}} \sum_{\mathbf{R}_i} \exp(i\mathbf{K} \cdot \mathbf{R}_i) \Phi(\mathbf{r} - \mathbf{R}_i), \quad (6)$$

where χ_σ is the standard spin (up or down) component of the Bloch function, $N=4p$ is the number of the lattice sites contained in the length of one period along the axis of the ZSWCNT ($p, 0$), \mathbf{R}_i is the position vector of the i th carbon atom, \mathbf{K} is the wave vector of the K point, which is given by

$$\mathbf{K} = \frac{2\pi}{a_0} \left(\mathbf{e}_x \frac{1}{3} + \mathbf{e}_y \frac{1}{\sqrt{3}} \right), \quad (7)$$

$F_{\nu\lambda}(\mathbf{r})$ is the smoothly varying envelope function, which can be written in the two-component form^{37,39}

$$F_{\nu\lambda}(\mathbf{r}) = \frac{1}{\sqrt{AL}} \exp(i\mathbf{k} \cdot \mathbf{r}) \frac{1}{\sqrt{2}} \begin{pmatrix} \frac{\kappa_{\nu m} - ik}{\sqrt{\kappa_{\nu m}^2 + k^2}} \\ s \end{pmatrix}, \quad (8)$$

\mathbf{k} is the two-dimensional wave vector counted from the K point

$$\mathbf{k} = \mathbf{e}_x \kappa_{vm} + \mathbf{e}_y k, \quad (9)$$

\mathbf{e}_x and \mathbf{e}_y being the unit vectors of the x and y axes, respectively.

Inserting Eq. (6) into Eq. (5) and bearing in mind that near the lattice sites \mathbf{R}_i the Wannier functions $\Phi(\mathbf{r}-\mathbf{R}_i)$ differ only slightly from the atomic functions $\phi(\mathbf{r}-\mathbf{R}_i)$, we can express the matrix element $V_{a\sigma, \nu\lambda\sigma}$ in the form

$$V_{a\sigma, \nu\lambda\sigma} = \frac{1}{\sqrt{N}} \sum_{\mathbf{R}_i} \exp(i\mathbf{K} \cdot \mathbf{R}_i) F_{\nu\lambda}(\mathbf{R}_i) \times \int \Psi_{a\sigma}^*(\mathbf{r}) V(\mathbf{r}-\mathbf{R}_a) \phi(\mathbf{r}-\mathbf{R}_i) d^3r, \quad (10)$$

where we have set the function $F_{\nu\lambda}$ outside the integral sign because the envelope function is a slowly varying function on the scale of a unit cell. Assuming that only one adatom and two nearest-neighbor carbon atoms are involved in the SWCNT-adatom interaction and using Eq. (10), we obtain

$$|V_{a\sigma, \nu\lambda\sigma}|^2 = \frac{4|V_0|^2}{NAL} \cos^2 \left[\frac{(\mathbf{K} + \mathbf{k})\mathbf{d}}{2} \right], \quad (11)$$

where we have introduced the interaction parameter

$$V_0(\mathbf{R}_a) = \int \Psi_{a\sigma}^*(\mathbf{r}) V(\mathbf{r}-\mathbf{R}_a) \phi(\mathbf{r}) d^3r, \quad (12)$$

which describes an effective coupling between the adatom and the SWCNT. Its precise assessment is a rather difficult and, what is more, somewhat ambiguous task because neither an effective self-consistent Hartree-Fock potential $V(\mathbf{r}-\mathbf{R}_a)$ nor an equilibrium distance \mathbf{R}_a between the adatom and the nanotube are known. Therefore, rather than calculate V_0 from first principles, we shall treat it, in agreement with the general philosophy of the Anderson-Newns approach,^{31,32} as a phenomenological parameter, using the fitting procedure to obtain its value relevant to the adsorption of atomic oxygen on SWCNTs (see Sec. III).

Comparison of the above expression for $|V_{a\sigma, \nu\lambda\sigma}|^2$ with that obtained in Ref. 30 for the atop binding shows that the effective strength of the interaction, induced by electronic shuttling between the adatom and the substrate ZSWCNT, is augmented by a factor 4 in the case of the bridge binding. Moreover, as seen from equation Eq. (11), the adatom in the bridge position generates a new factor of the form $\cos^2[(\mathbf{K} + \mathbf{k})\mathbf{d}/2]$ in the expression for $|V_{a\sigma, \nu\lambda\sigma}|^2$, which reinforces the contribution to the interaction originating from the states near the $K(K')$ points. The appearance of this weight factor is just what one could expect in the case of bridge binding on the basis of the discussion in Ref. 41.

Using Eqs. (7) and (9), we can specialize Eq. (11) to the case of bridge binding in position I and in position II. For the former it transforms into

$$|V_{a\sigma, \nu\lambda\sigma}^I|^2 = \frac{4|V_0|^2}{NAL} \cos^2 \left(\frac{kd}{2} + \frac{\pi}{3} \right), \quad (13)$$

while for the latter it takes the form

$$|V_{a\sigma, \nu\lambda\sigma}^{II}|^2 = \frac{4|V_0|^2}{NAL} \cos^2 \left[(k + \sqrt{3}\kappa_{vm}) \frac{d}{4} + \frac{\pi}{3} \right]. \quad (14)$$

As we shall see further, the difference between these two expressions is only of minor importance and manifests itself physically in but slightly different binding energies on the specific adsorption sites considered.

All information relevant to the adatom binding is contained entirely in the adatom Green's function $G_{aa}^\sigma(\varepsilon)$, which represents the propagator associated with an adatom electron and is, therefore, the key to calculate the adsorption energy. Constructing the Green's function according to the Anderson-Newns model yields

$$G_{aa}^\sigma(\varepsilon) = [\varepsilon - E_{a\sigma} - \Delta_a^{(\nu)}(\varepsilon) + i\Lambda_a^{(\nu)}(\varepsilon)]^{-1}, \quad (15)$$

where the so-called chemisorption functions $\Delta_a^{(\nu)}(\varepsilon)$ and $\Lambda_a^{(\nu)}(\varepsilon)$ are defined by

$$\Delta_a^{(\nu)}(\varepsilon) = \pi \sum_{J=K, K'} \sum_{\lambda, \sigma} |V_{a\sigma, \nu\lambda\sigma}|^2 \delta(\varepsilon - \varepsilon_{\nu\lambda}^{(J)}), \quad (16)$$

$$\Lambda_a^{(\nu)}(\varepsilon) = \frac{1}{\pi} P \int_{-\infty}^{\infty} \frac{\Delta_a^{(\nu)}(\varepsilon')}{\varepsilon - \varepsilon'} d\varepsilon'. \quad (17)$$

Here the symbol P stands for the Cauchy principle value. The physical meaning of $\Delta_a^{(\nu)}(\varepsilon)$ and $\Lambda_a^{(\nu)}(\varepsilon)$ is quite clear: $\Lambda_a^{(\nu)}(\varepsilon)$ is the shift of the adatom level, whereas $\Delta_a^{(\nu)}(\varepsilon)$ is half its width.

Within the simple band model of the ZSWCNTs we have adopted, the calculation of both the functions $\Delta_a^{(\nu)}(\varepsilon)$ and $\Lambda_a^{(\nu)}(\varepsilon)$ can be carried out exactly. For convenience we scale all energies with γ and introduce the notation $E = \varepsilon/\eta$ and $E_{vm} = \varepsilon_{vm}/\eta$. Inserting Eqs. (2), (13), and (14) into Eq. (16) and making use of the substitution

$$\sum_k \rightarrow \frac{A}{2\pi} \int_{-\infty}^{\infty} dk, \quad (18)$$

which is valid in the limit when the length of the nanotube goes to infinity, we obtain

$$\frac{\Delta_a^{(\nu)}(E)}{\eta} = \frac{4\sqrt{3}}{\pi} B^2 \sum_{m=-(p-1)}^{p-1} D(E, E_{vm}) \times [1 - W^{I,II}(E, E_{vm})], \quad (19)$$

where $B = |V_0|/|V_{pp\pi}|$ is the dimensionless coupling constant between the adatom and the SWCNT,

$$D(E, E_{vm}) = \begin{cases} \frac{|E|}{\sqrt{E^2 - E_{vm}^2}} & \text{for } |E| > |E_{vm}|, \\ 0 & \text{for } |E| < |E_{vm}|, \end{cases} \quad (20)$$

and the m sum runs over the occupied valence band states. In Eq. (19), we have also used the following notation:

$$W^{I,II}(E, E_{vm}) = \begin{cases} \frac{1}{2} \cos\left(\frac{2\pi}{3\sqrt{3}p} \sqrt{E^2 - E_{vm}^2}\right) & \text{(I),} \\ \cos\left(\frac{\pi}{3p} E_{vm} - \frac{\pi}{3}\right) \times \cos\left(\frac{\pi}{3\sqrt{3}p} \sqrt{E^2 - E_{vm}^2}\right) & \text{(II),} \end{cases} \quad (21)$$

where the superscripts I and II refer to bridge positions I and II, respectively.

Use of Eq. (19) in Eq. (17) yields

$$\frac{\Lambda_a^{(v)}(E)}{\eta} = -\frac{4\sqrt{3}}{\pi} B^2 \left[\delta_{v0} P^{I,II}(E) + \sum_{m=-(p-1)}^{p-1} (1 - \delta_{v0} \delta_{m0}) Q^{I,II}(E, E_{vm}) \right] \quad (22)$$

with δ_{ab} denoting the Kronecker delta symbol. The functions $P^{I,II}(E)$ and $Q^{I,II}(E, E_{vm})$ are defined separately for bridge positions I and II. For the former case they are given by

$$P^I(E) = \frac{1}{2} \sin\left(\frac{2\pi}{3\sqrt{3}p} E\right), \quad (23)$$

$$Q^I(E, E_{vm}) = \begin{cases} \frac{E}{\sqrt{E_{vm}^2 - E^2}} \left[1 - \frac{1}{2} \exp\left(-\frac{2\pi}{3\sqrt{3}p} \sqrt{E_{vm}^2 - E^2}\right) \right] & \text{for } |E| < |E_{vm}|, \\ \frac{E}{2\sqrt{E^2 - E_{vm}^2}} \sin\left(\frac{2\pi}{3\sqrt{3}p} \sqrt{E^2 - E_{vm}^2}\right) & \text{for } |E| > |E_{vm}|, \end{cases} \quad (24)$$

whereas for the latter case they take the form

$$P^{II}(E) = \frac{1}{2} \sin\left(\frac{\pi}{3\sqrt{3}p} E\right), \quad (25)$$

$$Q^{II}(E, E_{vm}) = \begin{cases} \frac{E}{\sqrt{E_{vm}^2 - E^2}} \left[1 - \cos\left(\frac{\pi}{3p} E_{vm} - \frac{\pi}{3}\right) \exp\left(-\frac{\pi}{3\sqrt{3}p} \sqrt{E_{vm}^2 - E^2}\right) \right] & \text{for } |E| < |E_{vm}|, \\ \frac{E}{\sqrt{E^2 - E_{vm}^2}} \cos\left(\frac{\pi}{3p} E_{vm} - \frac{\pi}{3}\right) \sin\left(\frac{\pi}{3\sqrt{3}p} \sqrt{E^2 - E_{vm}^2}\right) & \text{for } |E| > |E_{vm}|. \end{cases} \quad (26)$$

We now proceed to the determination of the adsorption energy ΔE_{ads} . Our starting point for a calculation of this quantity is the following expression for ΔE_{ads} in terms of the change in the one-electron energy $\Delta E_{1\sigma}$ upon adsorption:^{31,33}

$$\Delta E_{\text{ads}} = \sum_{\sigma} \Delta E_{1\sigma} - U \langle n_{a\sigma} \rangle \langle n_{a-\sigma} \rangle - \varepsilon_a - V_{\text{im}}^{\text{eff}} \quad (27)$$

with

$$\Delta E_{1\sigma} = \varepsilon_{l\sigma} + \frac{1}{\pi} \int_{-\infty}^{\mu_{\nu}} g_c(\varepsilon) \tan^{-1} \left[\frac{\Delta_a^{(v)}(\varepsilon)}{\varepsilon - E_{a\sigma} - \Lambda_a^{(v)}(\varepsilon)} \right] d\varepsilon, \quad (28)$$

where the upper limit of the integral is

$$\mu_{\nu} = (-\gamma/3R) \delta_{\nu, \pm 1}, \quad (29)$$

and the first term on the right-hand side of Eq. (28) takes into account the possibility of the occurrence of a truly localized state created by an adatom, whose energy $\varepsilon_{l\sigma}$ falls into the band gap of the semiconducting ZSWCNTs. We have introduced a cutoff function $g_c(\varepsilon)$ into the integrand of Eq. (28) in

order to eliminate the contribution to the integral arising from the electronic states lying outside the vicinity of the K and K' points, where the $\mathbf{k} \cdot \mathbf{p}$ model used is not valid. We choose this function in the form similar to (but not identical) that suggested in Ref. 39:

$$g_c(\varepsilon) = \frac{\varepsilon_c^2}{(0.15\varepsilon)^2 + \varepsilon_c^2}. \quad (30)$$

Here the parameter ε_c represents a cutoff energy and is chosen to be equal to γk_c with the cutoff wave number $k_c = \delta_c (2\pi/a_0)$, where the parameter δ_c is about 0.1–0.2. Such a choice of the artificial cutoff function is, certainly, rather arbitrary and cannot be justified *a priori*. Further we will illustrate how the results of the actual calculations of the adsorption energy and charge transfer in the problem at hand depend on the choice of the value of δ_c in the abovementioned interval.⁴²

One more comment is in place with regard to Eq. (27). The presence of the term $V_{\text{im}}^{\text{eff}}$ in this equation, which takes account of the interaction between the ion core of the adsor-

bate and the SWCNT, implies that the chemisorption process we treat here is not of purely electronic origin. It follows from Eq. (27) that it is necessary to consider the average electron occupation number of the adatom orbital $|a\sigma\rangle$, which is

$$\langle n_{a\sigma} \rangle = \int_{-\infty}^{\mu_\nu} \rho_a^\sigma(\varepsilon) g_c(\varepsilon) d\varepsilon + \delta_{\nu,\pm 1} \langle n_{a\sigma} \rangle_l, \quad (31)$$

where

$$\rho_a^\sigma(\varepsilon) = -\frac{1}{\pi} \text{Im} G_{aa}^\sigma(\varepsilon) = \frac{1}{\pi} \frac{\Delta_a^{(\nu)}(\varepsilon)}{[\varepsilon - E_{a\sigma} - \Lambda_a^{(\nu)}(\varepsilon)]^2 + [\Delta_a^{(\nu)}(\varepsilon)t]^2} \quad (32)$$

is the projected density of states for the adatom orbital and $\langle n_{a\sigma} \rangle_l$ is the occupancy of the localized-gap state associated with the adatom, which is determined by the residue of the Green's function $G_{aa}^\sigma(\varepsilon)$ at $\varepsilon = \varepsilon_{l\sigma}$, that is,

$$\langle n_{a\sigma} \rangle_l = [1 - \partial \Lambda_a^{(\nu=\pm 1)}(\varepsilon) / \partial \varepsilon]_{\varepsilon=\varepsilon_{l\sigma}}^{-1}. \quad (33)$$

Here the localized state energy $\varepsilon_{l\sigma}$ is given by the poles of the adatom Green's function (15) and, as such, is obtained from the equation

$$\varepsilon - E_{a\sigma} - \Lambda_a^{(\nu=\pm 1)}(\varepsilon) = 0, \quad (34)$$

since for the semiconducting ZSWCNTs the chemisorption function $\Delta_a^{(\nu=\pm 1)}(\varepsilon) = 0$ outside the bands of allowed energies [see Eqs. (19) and (20)]. If Eq. (34) has a solution $\varepsilon = \varepsilon_{l\sigma}$, this is a real discrete level, so that the corresponding level density is

$$\rho_{al}^\sigma(\varepsilon) = \langle n_{a\sigma} \rangle_l \delta(\varepsilon - \varepsilon_{l\sigma}). \quad (35)$$

According to Eq. (31), the occupancy $\langle n_{a\sigma} \rangle$ via $E_{a\sigma}$ is a function of $\langle n_{a-\sigma} \rangle$,

$$\langle n_{a\sigma} \rangle = f(\langle n_{a-\sigma} \rangle). \quad (36)$$

On changing $\sigma \rightarrow -\sigma$, this equation gives $\langle n_{a-\sigma} \rangle$ as a function of $\langle n_{a\sigma} \rangle$,

$$\langle n_{a-\sigma} \rangle = f(\langle n_{a\sigma} \rangle). \quad (37)$$

The self-consistency condition to determine both the averages in Eqs. (36) and (37) is given by

$$f[f(\langle n_{a\sigma} \rangle)] - \langle n_{a\sigma} \rangle = 0, \quad (38)$$

and we can see that there always exist a “nonmagnetic” solution of this equation, which corresponds to the equal values of $\langle n_{a\sigma} \rangle$ and $\langle n_{a-\sigma} \rangle$. If such a solution is obtained, then we can calculate the chemisorption energy ΔE_{ads} using Eq. (27), as well as the charge transfer from the substrate ZSWCNT to the adatom, which is

$$\Delta q/e = 2\langle n_{a\sigma} \rangle - 1 \quad (39)$$

(e is the electron charge).

III. NUMERICAL RESULTS AND DISCUSSION

In this section we are concerned with the application of the formalism developed above to the case of atomic oxygen

chemisorption on a series of ZSWCNTs $(p, 0)$ with p ranging from 9 to 18, that corresponds to the variation of the nanotube diameter from 0.7 to 1.4 nm. We present numerical examples of both the chemisorption functions $\Delta_a^{(\nu)}(\varepsilon)$ and $\Lambda_a^{(\nu)}(\varepsilon)$ as well as the adsorbate spectral density $\rho_a^\sigma(\varepsilon)$, and calculate chemisorption energies of a single O atom on the outer surface of the nanotubes. We also evaluate the charge transfer from the nanotubes to the adatom.

To carry out the calculations, we first of all need to specify the values of the essential parameters that describe our model. The latter is characterized for the adatom by the electron level ε_a and the intra-atomic Coulomb parameter U , and for the SWCNTs by the band parameter γ and the Fermi energy E_F . As has already been mentioned, E_F is taken to be the zero-energy reference. Assuming that $V_{pp\pi} = -3$ eV, which is a representative value for SWCNT,³⁸ we obtain $\gamma = 6.39$ eV Å. In order to choose the appropriate values of ε_a and U , we can make use of the relations⁴³

$$\varepsilon_a = \varphi - I, \quad U = I - A_0, \quad (40)$$

where φ is the SWCNT work function, I is the first ionization potential, and A_0 is the electron affinity. The latter two quantities for an isolated O atom are well known (see, e.g., Ref. 44) and equal to 13.6 and 1.5 eV, respectively. Throughout our calculations we keep the parameter φ fixed at the value $\varphi = 4.8$ eV,⁴⁵ since there is no reason to believe that it varies significantly from one tube to another within the given series of the $(p, 0)$ tubes with $p = 9-18$. Thus, we take $\varepsilon_a = -8.8$ eV and $U = 12.1$ eV.

According to the conceptual picture of the adsorption, suggested by the Anderson-Newns type of model we adopted, the two remaining parameters of the model $V_{\text{im}}^{\text{eff}}$ and V_0 describe, respectively, the ionic and the electronic components of the interaction between the adsorbate and the substrate ZSWCNT. The accurate evaluation of both these parameters goes beyond the Anderson-Newns model itself. One possible way to roughly estimate these parameters might be adjusting them to give the best fit to experimentally derived binding energy of a single O atom on the surface of even one ZSWCNT under consideration. However, it is not currently feasible to use this method, since we are not aware of any such experimental data. Therefore, we will follow a somewhat different path in order to determine the proper values of $V_{\text{im}}^{\text{eff}}$ and V_0 , namely, we will adjust the parameter set so that the calculated adsorption energies of the adatom on the ZSWCNTs will tend towards the value of about -2.1 eV with increasing the nanotube radius. The latter value is chosen as a representative one for the chemisorption energy of an oxygen atom on a graphene plane. This value is in the middle between the value of -1.73 eV obtained by Incze *et al.*^{46,47} from the first-principles calculations of the single-oxygen adsorption energy on the basal (0001) graphite surface at the lowest oxygen coverage of 5.5% and the value of -2.41 eV calculated by Fromherz *et al.*⁴⁸ for the bridge bonded O on a cluster-model graphite surface by using the semiempirical MINDO/3 method. Having performed a number of simulations by varying $V_{\text{im}}^{\text{eff}}$ and V_0 within a reasonable energy range, we have made sure that a correct asymptotic

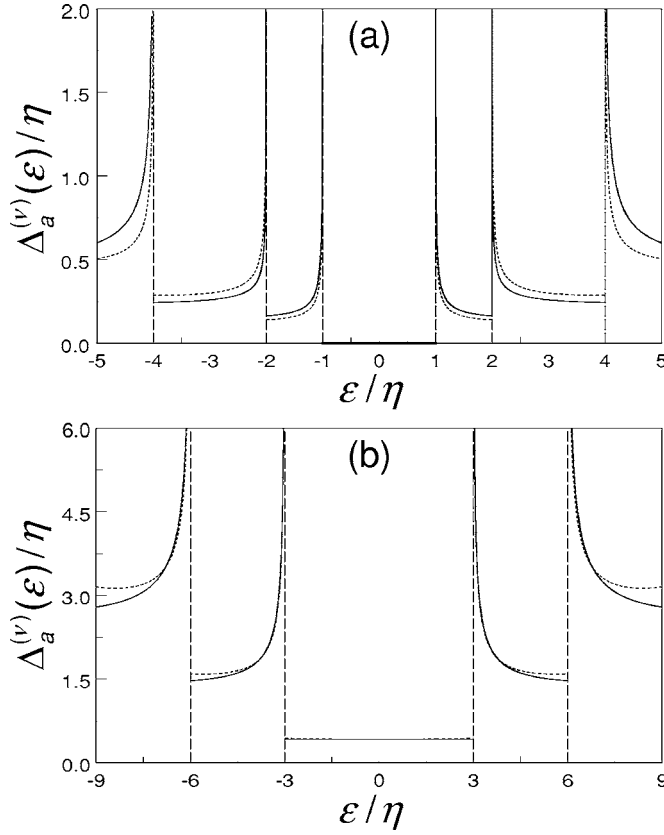


FIG. 2. Plot of the chemisorption function $\Delta_a^{(v)}(\varepsilon)$ defined in Eq. (19) for a semiconducting ZSWCNT (10,0) (a) and for a metallic one (12,0) (b). Dotted (full) curves correspond to bridge position I(II) of an adatom on the surface of the nanotubes. The dimensionless hopping parameter B is 0.33.

behavior of ΔE_{ads} is achieved by setting the parameters $V_{\text{im}}^{\text{eff}}$ and V_0 to be equal to 0.89 and 1.5 eV, respectively, which are the values we will use in what follows. It should be noted, however, that despite these values seem to be reasonable, the fitting procedure, we were forced to resort to, is, certainly, somewhat ambiguous, since we handled the two parameters to fit a single number (binding to a graphene plane). Whether our choice of the values of the parameters is correct can only be answered on the basis of the comparison of the adsorption energies inferred from experiments, if available, with those computed using the theory developed above. On the other hand, we wish to emphasize yet again that our goal here is not to predict the adsorption energy with extreme accuracy but rather to gain an insight into the physical origin of systematic qualitative chemisorption energy trends.

Once the main parameters entering the model are chosen, the calculation of $\Delta q/e$ and ΔE_{ads} is a tedious but straightforward process which involves the following steps.

(1) Calculation of the effective adsorbate level $E_{a\sigma}$ by using Eq. (1), where the occupancy $\langle n_{a-\sigma} \rangle$ is taken as a variable parameter which runs from 0 to 1. To obtain $E_{a\sigma}$ as a function of $\langle n_{a-\sigma} \rangle$ with good accuracy, it is sufficient to use a grid of approximately 10^3 evenly spaced values of $\langle n_{a-\sigma} \rangle$ from the abovementioned interval.

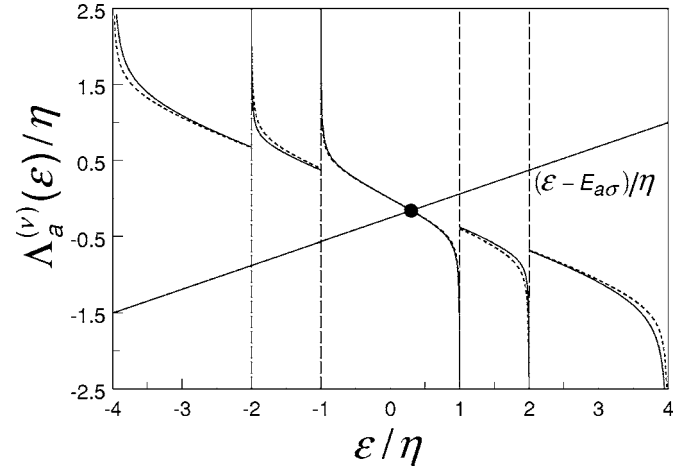


FIG. 3. Plot of the chemisorption function $\Delta_a^{(v)}(E)$ defined in Eq. (22) for a semiconducting ZSWCNT (10,0). Dotted (full) curves correspond to bridge position I(II) of an adatom on the surface of the nanotube. Parameter B is the same as in Fig. 2. The intersection with a slanting straight line $(\varepsilon - E_{a\sigma})/\eta$, marked with a solid dot gives the solution of Eq. (34) for the localized state energy $\varepsilon_{l\sigma}$.

(2) Calculation of the chemisorption functions $\Delta_a^{(v)}(\varepsilon)$ and $\Lambda_a^{(v)}(\varepsilon)$ according to Eqs. (19) and (22), respectively.

(3) Calculation of the adsorbate spectral density $\rho_a^{\sigma}(\varepsilon)$ by using Eq. (32).

(4) Solution of Eq. (34), which yields the localized state energies $\varepsilon_{l\sigma}$ lying in the band gap of the semiconducting SWCNTs, and calculation of the average occupation numbers $\langle n_{a\sigma} \rangle_l$ of those states by means of Eq. (33).

(5) Calculation of the occupancy $\langle n_{a\sigma} \rangle$ of the adatom orbital $|a\sigma\rangle$ as a function $\langle n_{a-\sigma} \rangle$ by evaluating the integral in Eq. (31).

(6) Numerical solution of Eqs. (36) and (37) in a self-consistent manner, as prescribed by Eq. (38). The last equation can roughly be solved graphically by looking for the intersections of the two curves obtained on plotting $\langle n_{a\sigma} \rangle$ against $\langle n_{a-\sigma} \rangle$ and vice versa.⁴⁹ The rout of Eq. (38) thus obtained is then defined more exactly by using the bisection method.

(7) Calculation of $\Delta q/e$ and ΔE_{ads} according to Eqs. (39) and (27), respectively, using the self-consistent value of $\langle n_{a\sigma} \rangle$ obtained in the preceding item.

On the basis of the numerical calculations, implemented as outlined above, we obtain the results presented in Figs. 2–9, which we discuss next. Figure 2 gives a plot of the dimensionless chemisorption function $\Delta_a^{(v)}(E)/\eta$ versus the dimensionless energy $E = \varepsilon/\eta$ for two different ZSWCNTs: semiconducting (10,0) [Fig. 2(a)] and metallic (12,0) [Fig. 2(b)]. As seen from this figure, the behavior of $\Delta_a^{(v)}(E)$ for both nanotubes closely resembles that of the density of states for the same nanotubes.³⁸ In particular, several pronounced peaks of $\Delta_a^{(v)}(E)$ are observed at the size-quantized energy subband edges, which are related to the square-root van Hove singularities in the density of states at $|E| = |E_{vm}|$ for $E_{vm} \neq 0$. The overall picture of the dependence of $\Delta_a^{(v)}$ on E is similar to that we observed in the on-top chemisorption

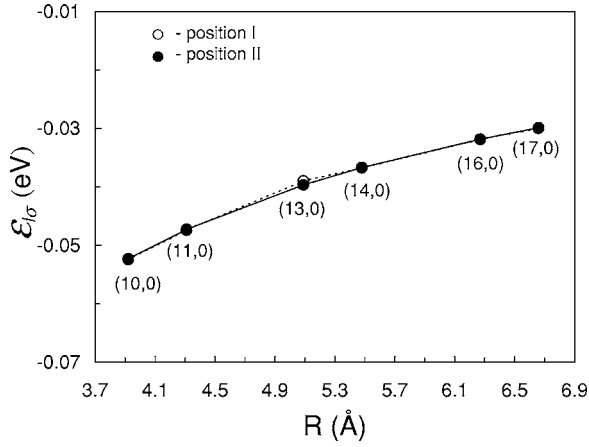


FIG. 4. Localized state energies $\varepsilon_{l\sigma}$ for several semiconducting ZSWCNTs as a function of the nanotube radius R . Open (solid) dots correspond to bridge position I (II) of an adatom on the surface of the nanotubes. These energies are calculated from Eq. (34) using the self-consistent values of $\langle n_{a\sigma} \rangle$ obtained for each tube as explained in the text. The numbers in parenthesis stand for the tube chirality indices. The solid and dashed lines are intended as a guide to the eye.

model developed in Ref. 30, where $\Delta_a^{(v)}(E)$ is expressed in terms of the only function $D(E, E_{vm})$ defined by Eq. (20), and as such preserves the concise form of the density of states for ZSWCNTs.⁵⁰ We also note that there is no significant difference between the $\Delta_a^{(v)}(E)$ curves referring to the two different bridge positions under consideration, and only at large values of E slight differences begin to emerge on the wings of the peaks of $\Delta_a^{(v)}(E)$. These differences are, however, of minor importance in evaluating the total chemisorption energy ΔE_{ads} . The reason for this is that large values of E are excluded from the integrand of Eq. (28) due to the presence of the cutoff function $g_c(\varepsilon)$ in that equation.

Figure 3 typifies a common behavior of the chemisorption function $\Lambda_a^{(v)}(E)$ for semiconducting ZSWCNTs. According

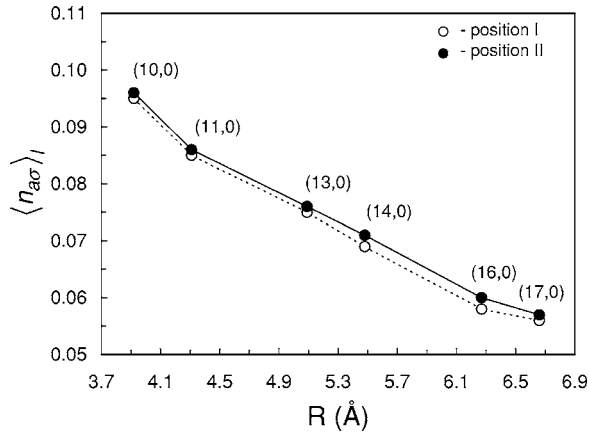


FIG. 5. Mean occupation numbers $\langle n_{a\sigma} \rangle_l$ of the localized states, whose energies are presented in Fig. 4, versus the nanotube radius R . Open (solid) dots correspond to bridge position I (II) of an adatom on the surface of the nanotubes. The numbers in parenthesis stand for the tube chirality indices. The solid and dashed lines are intended as a guide to the eye.

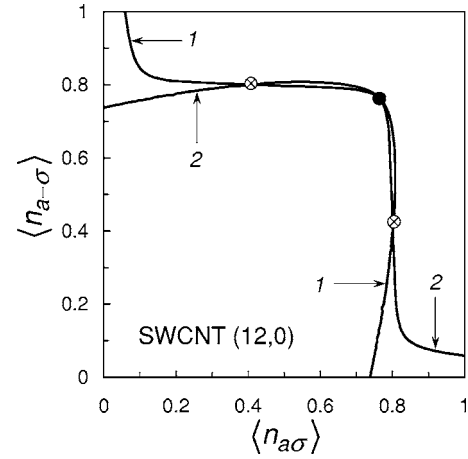


FIG. 6. Example of a graphical solution of Eq. (38) for the O adatom adsorbed in position II on the surface of a ZSWCNT (12, 0). The intersection points of curves 1 and 2 give a “nonmagnetic” root of Eq. (38) (marked with a heavy dot) and a pair of “magnetic” roots of the same equation (marked with crosses).

to Eq. (17), this function is the Hilbert transform of the function $\Delta_a^{(v)}(E)$ and as such exhibits divergent singularities just at the same points as the function $\Delta_a^{(v)}(E)$. The only difference is that $\Lambda_a^{(v)}(E)$ is divergent in $1/\sqrt{E_{vm}-E}$ form, whereas $\Delta_a^{(v)}(E)$ diverges in reverse $1/\sqrt{E-E_{vm}}$ form. Figure 3 is also

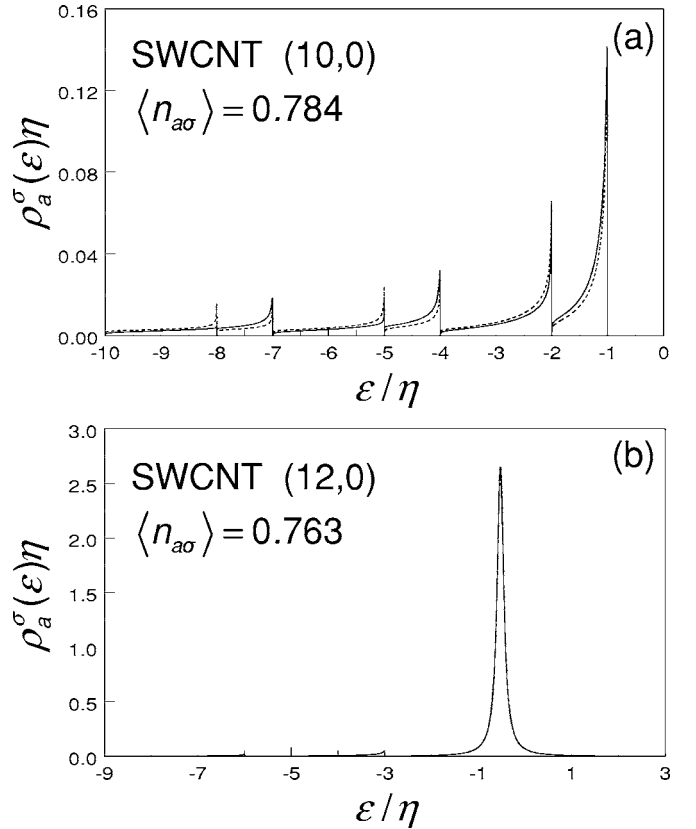


FIG. 7. Adatom density of states $\rho_a^\sigma(\varepsilon)$ defined in Eq. (32) for a semiconducting ZSWCNT (10,0) (a) and for a metallic one (12,0) (b). Dotted (full) curves correspond to bridge position I(II) of an adatom on the surface of the nanotubes.

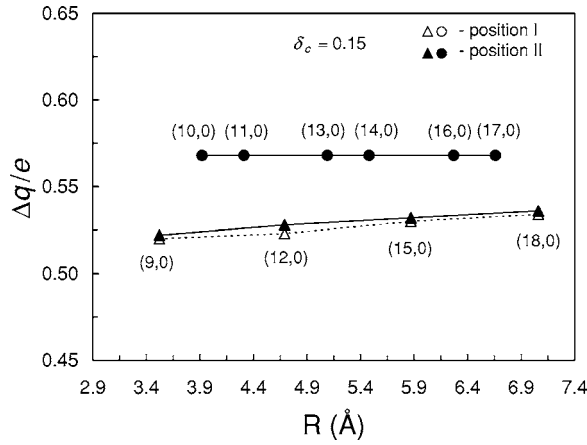


FIG. 8. Charge transfer $\Delta q/e$ from the ZSWCNTs $(p,0)$ with $p=9-18$ to the O atom adsorbed in bridge position I (open symbols) and bridge position II (solid symbols) as a function of the nanotube radius R . The cutoff parameter δ_c is chosen to be equal to 0.15. The dots and the triangles refer to semiconducting and metallic ZSWCNTs, respectively. The numbers in parenthesis stand for the tube chirality indices. The solid and dashed lines are intended as a guide to the eye.

an example of how the solution of Eq. (31) for localized state energies can be obtained graphically. From the monotonic variation of $\Lambda_a^{(v)}(E)$ from $+\infty$ to $-\infty$ inside the band gap of semiconducting ZSWCNTs, it is evident that at least one localized state always exists. The energy and the occupancy of this state for the different semiconducting ZSWCNTs under consideration are plotted in Figs. 4 and 5, respectively, as a function of the nanotube radius. We remind the reader that throughout our calculations, the Fermi level is taken as the zero of energy so that the localized state energies in Fig. 4 lie entirely in the lower half of the band gap. Bearing this point in mind, we may identify the localized states under consideration as acceptor ones. As such, they can provide an effec-

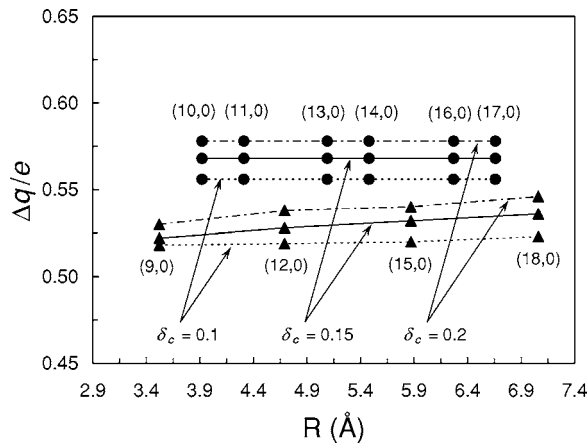


FIG. 9. Charge transfer $\Delta q/e$ from the ZSWCNTs $(p,0)$ with $p=9-18$ to the O atom adsorbed in bridge position II as a function of the nanotube radius R for three different values of the cutoff parameter δ_c : 0.1, 0.15, and 0.2. The solid, dashed, and dot-dashed lines are intended as a guide to the eye. Other notations are the same as in Fig. 8.

tive means of altering and tuning the electronic and transport properties of the nanotubes, as is the case for conventional semiconductors doped by acceptor impurities. For the problem at hand, these states also play an important role. As can be seen from Fig. 4 in combination with Eq. (27), they directly lower the values of ΔE_{ads} (by about 0.1 eV) for the semiconducting tubes as compared with the metallic ones.

There is one more point to note regarding Figs. 4 and 5. Whether the adsorption occurs in position I or in position II has a minor influence on the localized state energies and their occupancies. Indeed, as seen from those figures, the energies $\varepsilon_{l\sigma}$ for both the abovementioned positions of the adatom practically coincide with one another, whereas the corresponding occupancies $\langle n_{a\sigma} \rangle_I$ in position I are different from those in position II, but only slightly. It should also be mentioned that the calculated mean occupation numbers $\langle n_{a\sigma} \rangle_I$ of the localized states are generally rather small, decreasing with increasing the nanotube radius. This implies that in the case of the single-oxygen-atom adsorption we are concerned with here, one can scarcely expect any drastic changes in the electronic properties of the nanotubes, produced by one of those states (see the theoretical results obtained by Rochefort and Avouris⁵¹ for the conductance of a SWCNT in which one carbon atom is substituted by one oxygen atom).

The results presented in Fig. 4 are obtained using the self-consistent values of $\langle n_{a\sigma} \rangle$, which, in turn, are calculated from Eq. (38). An example of the graphical solution of this equation is shown in Fig. 6 for a metallic ZSWCNT (12,0). The root of the equation, marked with a heavy dot in the figure, corresponds to a nonmagnetic state of the oxygen atom bonded to the nanotube, for which case $\langle n_{a\sigma} \rangle = \langle n_{a-\sigma} \rangle$. For our particular choice of the values of the relevant parameters of the model, a symmetrical pair of “magnetic” roots of Eq. (38), marked with crosses in Fig. 6, appears in addition to the “nonmagnetic” solution for all the examined ZSWCNTs, irrespective of their electronic structure. However, we are not going to treat these “magnetic” solutions, for which $\langle n_{a\sigma} \rangle \neq \langle n_{a-\sigma} \rangle$, since the Hartree-Fock approximation used in the Anderson-Newns approach is insufficient to give a proper treatment of the magnetic state of the system.⁵²

The curves of the adsorbate spectral density $\rho_a^\sigma(\varepsilon)$ are drawn in Figs. 7(a) and 7(b) for a semiconducting ZSWCNT (10,0) and a metallic one (12,0), respectively. The curves are calculated for the self-consistently determined values of $\langle n_{a\sigma} \rangle$ indicated in these figures. One can see that the overall behavior of ρ_a^σ as a function of E is similar to that observed in our previous work,³⁰ in which we dealt with the on-top chemisorption of a hydrogen atom on the outer surface of ZSWCNTs. In particular, a regular periodic pattern of sharply asymmetric Fano-like resonant peaks is clearly seen below the band gap of the semiconducting ZSWCNT [Fig. 7(a)]. These spectral features arise owing to the specific energy dependence of the chemisorption functions $\Delta_a^{(v)}(\varepsilon)$ and $\Lambda_a^{(v)}(\varepsilon)$ shown in Figs. 2 and 3, respectively. Thus, the abovementioned features are a direct consequence of the interaction between the discrete atomic state of the adsorbate and the quasicontinuum of the valence-band electronic states of the substrate ZSWCNT. As seen from Fig. 7(a), the spectral density $\rho_a^\sigma(\varepsilon)$ for both the considered positions of the adatom

exhibits zero points exactly at the edges of the size-quantized valence-energy subbands as well as the resonant peaks situated very close to these points. The differences between the shapes, as well as between the heights, of the position-I and position-II peaks are small, since the differences between the $\Delta_a^{(v)}(\epsilon)$ curves, as well as the $\Lambda_a^{(v)}(\epsilon)$ ones, for these two positions are also small. The same is true for the main resonant peak of $\rho_a^\sigma(\epsilon)$ in the case of metallic ZSWCNTs $(p,0)$, which has a Lorentzian shape and is located just below the Fermi level. Figure 7(b) demonstrates complete merging of the corresponding dependences ρ_a^σ on E for the two above-mentioned adsorption positions.

Figure 8 depicts the calculated charge transfer $\Delta q/e$ to the O adatom versus the nanotube radius R . As seen from this figure, the charge transfer for both semiconducting and metallic types of the ZSWCNTs changes only very little with R , being always larger for the former, for which $\Delta q/e$ remains at the level of about 0.55 independent of the nanotube radius and of the position of the adatom. Basically the same charge transfer, but a little smaller, is predicted by Fig. 8 for the metallic ZSWCNTs, for which case the adsorption position of the adatom does not at all manifest itself in the amount of electron transfer. Note that the above value 0.55 for the charge transfer is in reasonable agreement with the Mulliken-population-analysis value of 0.48 reported by Sorescu *et al.*¹⁴ for the charge transfer that occurs between a ZSWCNT (8,0) and a chemisorbed O atom. This result suggests that hole carriers can effectively be generated in the nanotubes upon the chemisorption of atomic oxygen, probably resulting in significant changes of their electronic properties—the point deserving thorough investigation but, certainly, being beyond the scope of the present paper.

Figure 9 illustrates the cutoff-energy dependence of the charge transfer to the adatom. The results shown in this figure refer to bridge position II of the adatom, but the same is true for position I as well. As seen from Fig. 9, the charge transfer becomes larger with an increase of the cutoff energy, but, on the whole, we can conclude that the charge transfer is not very sensitive to the δ_c value in the chosen interval $\delta_c = 0.1 - 0.2$.

In Fig. 10 we show the calculated values of the chemisorption energy ΔE_{ads} against the nanotube radius R . Note that, by definition, negative ΔE_{ads} values correspond to an energetically favorable adsorption. As seen from Fig. 10, the curves for ΔE_{ads} corresponding to both adsorption positions I and II have sawtooth shapes with the maxima corresponding to the metallic tubes. This implies that the binding of an oxygen atom to the semiconducting tubes is stronger than to the metallic ones, that correlates with larger charge transfer to the adatom from the former ones (see Fig. 8). One more important message of Fig. 10 is that in the case of the semiconducting tubes the ΔE_{ads} values is practically independent of the nanotube radius R , whereas for the metallic tubes ΔE_{ads} slightly decreases with increasing R , tending towards the “infinite” radius graphene case. Such a difference in the R -dependent behavior of ΔE_{ads} for these two types of tubes, as well as the lowering in ΔE_{ads} (by about 0.5 eV) for the semiconducting tubes as compared with the metallic ones, can be attributed to the contribution to ΔE_{ads} originating from the localized acceptor states created by the O adatom in

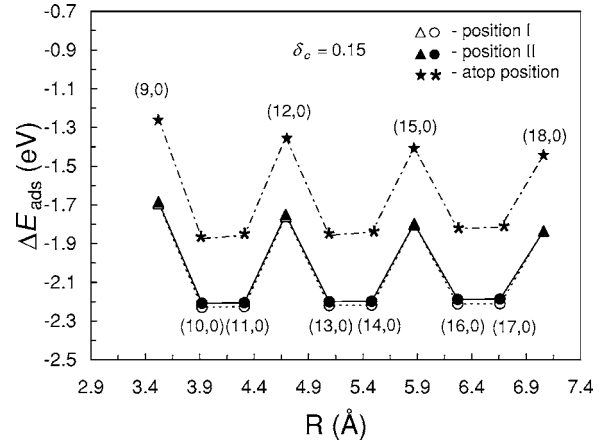


FIG. 10. Chemisorption energies ΔE_{ads} of a single O adatom on the surface of the ZSWCNTs $(p,0)$ with $p=9-18$ versus the nanotube radius R . The cutoff parameter δ_c is chosen to be equal to 0.15. The open (solid) dots as well as the open (solid) triangles refer to bridge position I (II). The dots and the triangles refer to semiconducting and metallic ZSWCNTs, respectively. The asterisks (*) and stars (★) show the results obtained for the O atom adsorbed directly on top of a surface carbon atom of semiconducting and metallic ZSWCNTs, respectively. The numbers in parenthesis stand for the tube chirality indices. The solid, dashed, and dot-dashed lines are intended as a guide to the eye.

the band gap of the semiconducting nanotubes. In this connection, it is worthwhile to note that both the first and the second terms in Eq. (27) for ΔE_{ads} in the case of semiconducting tubes depend on the characteristics of these states, namely, $\epsilon_{l\sigma}$ and $\langle n_{a\sigma} \rangle_l$ [see Eqs. (1) and (31)–(34)].

Although our main goal in this paper is to describe the chemisorption on the two C-C bridge sites (which, in accordance with previous *ab initio* studies, are preferable energetically), it would be of interest to see what our model predicts for the oxygen adsorption (i) directly above a C atom (atop site) and (ii) above the center of hexagonal carbon ring (hole site). At present we are able to discuss only case (i), for which the corresponding chemisorption functions $\Delta_a^{(v)}(\epsilon)$ and $\Lambda_a^{(v)}(\epsilon)$ were obtained in Ref. 30. A consideration of case (ii) would require a generalization of the above theory, which is beyond the scope of the present paper. The result obtained for case (i) are presented by asterisks and stars in Fig. 10 for semiconducting and metallic tubes, respectively. As can be seen from this figure, the adsorption energies on the atop site are about 0.5 eV higher than those in the bridge positions.

Finally, in Fig. 11 we illustrate the dependence of the adsorption energy ΔE_{ads} on the cutoff energy ϵ_c in the case of the chemisorption of the O adatom on bridge site II. As seen from this figure, the results are rather sensitive to the choice of the cutoff parameter δ_c . This means that the obtained adsorption energies may be used only to show how the electronic structure of ZSWCNTs affects qualitative chemisorption energy trends.

Turning back to Fig. 10, it is worthwhile to note another important result that follows from the graphs in this figure, namely, the chemisorption of a single O atom in both bridge positions I and II is equally probable from the energetic point

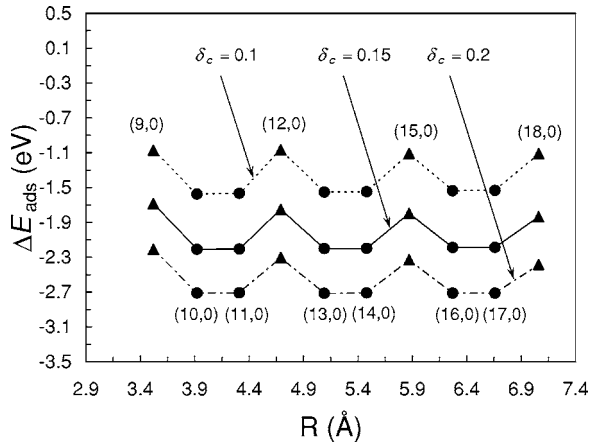


FIG. 11. Chemisorption energies ΔE_{ads} of a single O adatom adsorbed on the surface of the ZSWCNTs $(p,0)$ with $p=9-18$ in bridge position II as a function of the nanotube radius R for three different values of the cutoff parameter δ_c : 0.1, 0.15, and 0.2. The dots and the triangles refer to semiconducting and metallic ZSWCNTs, respectively. The numbers in parenthesis stand for the tube chirality indices. The solid, dashed and dot-dashed lines are intended as a guide to the eye.

of view as the corresponding adsorption energies are almost identical. To the best of our knowledge, there are no experimental data available at present, which would support or contradict this result. The lack of such data, as well as of single-atom-adsorption-energy measurements at all, undoubtedly reflects certain difficulties in the measurements. Nevertheless, as the experimental indications of bond formation between adsorbed species and substrate nanotubes can, in principle, be obtained by using different techniques, including photoelectron spectroscopy, atomic force microscopy, Raman spectroscopy and some others (see, e.g., Ref. 1), we hope that the present investigation will inspire experimentalists to test the theoretical predictions. This seems to be a difficult but feasible task.

IV. CONCLUSIONS

In this paper, we have developed a theory of atomic oxygen chemisorption on the outer surface of ZSWCNTs. The theory is based on the Anderson-Newns model, which idealizes the adatom to a single relevant electronic energy level and takes into account the intra-atomic Coulomb repulsion on the adatom. The one-electron band structure of the ZSWCNTs has been described by a simple $\mathbf{k} \cdot \mathbf{p}$ model within an effective-mass approximation. The screening-charge effect has been treated phenomenologically in terms of an image potential.

The fundamental result of the approach proposed here is the exact analytical expression for the adsorbate Green's

function, from which other important quantities characterizing chemisorption can be derived. Using a parametrization of the Anderson-Newns model as suggested by a matching of the calculated single-oxygen adsorption energies to give a correct result in the “infinite” radius graphene case, we have computed the chemisorption energy ΔE_{ads} of a single O atom on the sidewall of the ZSWCNTs $(p,0)$ with p ranging from 9 to 18, as well as the charge transfer $\Delta q/e$ between the nanotubes and the adatom. The obtained absolute values of ΔE_{ads} generally fall into the range 1.1–2.7 eV, exhibiting oscillatory jumplike behavior with changing the nanotube radius. Larger $|\Delta E_{\text{ads}}|$ values are shown to be associated with semiconducting tubes because of the contribution to ΔE_{ads} originating from the localized acceptor states produced by an O adatom in the band gap of such tubes. We have also found that the chemisorption of an O adatom on top of an axial C-C bond and on top of a zigzag C-C one is equally probable from the energetic point of view. In addition to this, it is shown that in any case the binding of an O adatom to the sidewall of the considered ZSWCNTs is accompanied by very significant charge transfer (of about 0.55 electron) directed from the tubes to the adatom, probably resulting in the generation of hole carriers in nanotubes. This result well agrees with the recent similar prediction by Sorescu *et al.*¹⁴ and suggests that drastic changes in the electronic transport properties of ZSWCNTs can be expected upon the chemisorption of atomic oxygen on their outer surface, which is of interest in device applications of the nanotubes.

In conclusion, the Anderson-Newns model employed in this paper offers a convenient physically motivated scheme for studying chemisorption of single oxygen atoms on the surface of ZSWCNTs. At present, our understanding of this issue still remains rather limited, and a relatively simple theory presented above may be useful for the development of physical insight. Although the theory does not claim to describe the chemisorption with accuracy that more sophisticated *ab initio* methods are able to provide, we believe that the knowledge obtained here should be borne in mind when results of more refined calculations are discussed.

ACKNOWLEDGMENTS

The authors would like to thank M. Burghard of the Max-Planck-Institut für Festkörperforschung (Stuttgart) for making available his review paper¹ on the chemical functionalization of SWCNTs. We are also grateful to R. N. Nazmutdinov of the Kazan State Technological University (Russia) for providing as with an electronic copy of his paper.⁴⁹ We are particularly indebted to the anonymous referee for his valuable and helpful comments. The support of the Ministry of Education of the Russian Federation through the program “Universities of Russia” (Grant No. 01.01.111) is gratefully acknowledged.

*Corresponding author. Postal address: Sovetskaya 31, kv. 32, Saransk 430000, Russia; Electronic address: 612033@inbox.ru

- ¹M. Burghard, *Surf. Sci. Rep.* **58**, 1 (2005).
- ²P. G. Collins, K. Bradley, M. Ishigami, and A. Zettl, *Science* **287**, 1801 (2000).
- ³G. U. Sumanasekera, C. Adu, S. Fang, and P. C. Eklund, *Phys. Rev. Lett.* **85**, 1096 (2000).
- ⁴K. Bradley, S. H. Jhi, P. G. Collins, J. Hone, M. L. Cohen, S. G. Louie, and A. Zettl, *Phys. Rev. Lett.* **85**, 4361 (2000).
- ⁵Ph. Avouris, *Acc. Chem. Res.* **35**, 1026 (2002).
- ⁶V. Derycke, R. Martel, J. Appenzeller, and Ph. Avouris, *Appl. Phys. Lett.* **80**, 2773 (2002).
- ⁷S. Heinze, J. Tersoff, R. Martel, V. Derycke, J. Appenzeller, and Ph. Avouris, *Phys. Rev. Lett.* **89**, 106801 (2002).
- ⁸H. Ulbricht, G. Moos, and T. Hertel, *Phys. Rev. B* **66**, 075404 (2002).
- ⁹A. Goldoni, R. Lorciprete, L. Petaccia, and S. Lizzit, *J. Am. Chem. Soc.* **125**, 11329 (2003).
- ¹⁰A. Goldoni, L. Petaccia, L. Gregoratti, B. Kaulich, A. Barinov, S. Lizzit, A. Laurita, L. Sangaletti, and R. Lorciprete, *Carbon* **42**, 2099 (2004).
- ¹¹S. Peng and K. Cho, *Nanotechnology* **11**, 57 (2000).
- ¹²S. H. Jhi, S. G. Louie, and M. L. Cohen, *Phys. Rev. Lett.* **85**, 1710 (2000).
- ¹³X. Y. Zhu, S. M. Lee, Y. H. Lee, and T. Frauenheim, *Phys. Rev. Lett.* **85**, 2757 (2000).
- ¹⁴D. C. Sorescu, K. D. Jordan, and Ph. Avouris, *J. Phys. Chem. B* **105**, 11227 (2001).
- ¹⁵N. Park, S. Han, and J. Ihm, *Phys. Rev. B* **64**, 125401 (2001).
- ¹⁶C. Y. Moon, Y. S. Kim, E. C. Lee, Y. G. Jin, and K. J. Chang, *Phys. Rev. B* **65**, 155401 (2002).
- ¹⁷J. Zhao, A. Buldum, J. Han, and J. P. Lu, *Nanotechnology* **13**, 195 (2002).
- ¹⁸A. Ricca and J. A. Drocco, *Chem. Phys. Lett.* **362**, 217 (2002).
- ¹⁹A. Ricca, C. W. Bauschlicher, and A. Maiti, *Phys. Rev. B* **68**, 035433 (2003).
- ²⁰S. P. Chan, G. Chen, X. G. Gong, and Z. F. Liu, *Phys. Rev. Lett.* **90**, 086403 (2003).
- ²¹P. Giannozzi, R. Car, and G. Scoles, *J. Chem. Phys.* **118**, 1003 (2003).
- ²²S. Dag, O. Gülseren, and S. Ciraci, *Chem. Phys. Lett.* **380**, 1 (2003).
- ²³Y.-F. Zhang and Z.-F. Liu, *J. Phys. Chem. B* **108**, 11435 (2004).
- ²⁴H. J. Liu and C. T. Chan, *Phys. Rev. B* **72**, 075437 (2005).
- ²⁵S. Dag, O. Gülseren, T. Yildirim, and S. Ciraci, *Phys. Rev. B* **67**, 165424 (2003).
- ²⁶G. E. Froudakis, M. Schnell, M. Mühlhäuser, S. D. Peyerimhoff, A. N. Andriotis, M. Menon, and R. M. Sheetz, *Phys. Rev. B* **68**, 115435 (2003).
- ²⁷V. Barone, J. Heyd, and G. E. Scuseria, *Chem. Phys. Lett.* **389**, 289 (2003).
- ²⁸S. P. Walch, *Chem. Phys. Lett.* **374**, 501 (2003).
- ²⁹D. J. Mann and M. D. Halls, *J. Chem. Phys.* **116**, 9014 (2002).
- ³⁰VL. A. Margulis, E. E. Muryumin, and O. B. Tomilin, *Physica B* **353**, 314 (2004).
- ³¹D. M. Newns, *Phys. Rev.* **178**, 1123 (1969).
- ³²P. W. Anderson, *Phys. Rev.* **124**, 41 (1961).
- ³³S. K. Lyo and R. Gomer, *Phys. Rev. B* **10**, 4161 (1974).
- ³⁴R. Gomer, *CRC Crit. Rev. Solid State Sci.* **4**, 247 (1974).
- ³⁵B. E. Granger, P. Král, H. R. Sadeghpour, and M. Shapiro, *Phys. Rev. Lett.* **89**, 135506 (2002).
- ³⁶M. Zamkov, H. S. Chakraborty, A. Habib, N. Woody, U. Thumm, and P. Richard, *Phys. Rev. B* **70**, 115419 (2004).
- ³⁷H. Ajiki and T. Ando, *J. Phys. Soc. Jpn.* **62**, 1255 (1993).
- ³⁸R. Saito, G. Dresselhaus, and M. S. Dresselhaus, *Physical Properties of Carbon Nanotubes* (Imperial College Press, London, 1998).
- ³⁹T. Ando, *J. Phys. Soc. Jpn.* **74**, 777 (2005).
- ⁴⁰U. Fano, *Phys. Rev.* **124**, 1866 (1961).
- ⁴¹T. L. Einstein, J. A. Hertz, and J. R. Schrieffer, in *Theory of Chemisorption*, edited by J. R. Smith (Springer, New York, 1980).
- ⁴²In our previous study (see Ref. 30) we did not address this critical issue, since $k_c = 2\pi/a_0$ has been used in that work.
- ⁴³J. W. Gadzuk, J. K. Hartman, and T. N. Rhodin, *Phys. Rev. B* **4**, 241 (1971).
- ⁴⁴D. M. Neumark, K. R. Lykke, T. Andersen, and W. C. Lineberger, *Phys. Rev. A* **32**, 1890 (1985).
- ⁴⁵V. Flip, D. Nicolaescu, and F. Okuyama, *J. Vac. Sci. Technol. B* **19**, 1016 (2001).
- ⁴⁶A. Incze, A. Pasturel, and C. Chatillon, *Appl. Surf. Sci.* **177**, 226 (2001).
- ⁴⁷A. Incze, A. Pasturel, and C. Chatillon, *Surf. Sci.* **537**, 55 (2003).
- ⁴⁸T. Fromherz, C. Mendoza, and F. Ruetz, *Mon. Not. R. Astron. Soc.* **263**, 851 (1993).
- ⁴⁹The comprehensive analysis of all possible routs of such an equation is given in: M. D. Bronshtein, R. N. Nazmutdinov, and W. Schmickler, *Chem. Phys. Lett.* **399**, 307 (2004), where the so-called wide band approximation is used. In this approximation $\Delta_a^{(v)}(\epsilon) = \Delta_0$ is independent of energy and $\rho_a^{\sigma}(\epsilon)$ is a simple Lorentzian of width Δ_0 centered around $E_{a\sigma}$.
- ⁵⁰J. W. Mintmire and C. T. White, *Phys. Rev. Lett.* **81**, 2506 (1998).
- ⁵¹A. Rochefort and Ph. Avouris, *J. Phys. Chem. A* **104**, 9807 (2000).
- ⁵²J. R. Schrieffer and D. C. Mattis, *Phys. Rev.* **140**, A1412 (1965).